2016

Nanoporous organosilicate thin films for sensing of vapor - phase analytes and comparison with nanoporous anodized aluminum oxide sensors

Rashmi Asalla

ABSTRACT

NANOPOROUS ORGANOSILICATE THIN FILMS FOR SENSING OF VAPOR- PHASE ANALYTES AND COMPARISON WITH NANOPOROUS ANODIZED ALUMINUM OXIDE SENSORS

Rashmi Asalla, MS
Department of Electrical Engineering
Northern Illinois University, 2016
Venumadhav Korampally, Director

Chemical sensors have been used in many industries from process control to monitoring the amount of gases in industries to environmental protection. Recent work showed that nanoporous anodized aluminum oxide (AAO) sensors were used to distinguish and discriminate alcohols and volatile organic compounds. It was also demonstrated that the impedance spectrum of these adsorbed analytes showed a unique trend. In this study nanoporous organosilicate films have shown promise as sensor substrates in detection of various vapor-phase analytes. We evaluated the properties of both hydrophobic and hydrophilic nanoporous organosilicate sensors using impedance spectroscopy (IS) to obtain the sensor response in time - domain and real and imaginary impedance of the sensor in various vapor - phase analytes. This work addresses the use of nanoporous organosilicate thin films as a low-cost alternative sensor substrate to nanoporous anodized aluminum oxide sensors. With this study it also showed that application of nanoporous organosilicate thin film can be further expanded as sensing devices for both industrial and commercial purposes.

NORTHERN ILLINOIS UNIVERSITY

DE KALB, ILLINOIS

DECEMBER 2016

NANOPOROUS ORGANOSILICATE THIN FILMS FOR SENSING OF VAPOR - PHASE ANALYTES AND COMPARISON WITH NANOPOROUS ANODIZED ALUMINUM OXIDE SENSORS

BY

RASHMI ASALLA

A THESIS SUBMITTED TO THE GRADUATE SCHOOL
IN PARTIAL FULFILLMENT OF THE REQUIREMENTS
FOR THE DEGREE
MASTER OF SCIENCE

DEPARTMENT OF ELECTRICAL ENGINEERING

Thesis Director:
Venumadhav Korampally

ACKNOWLEDGEMENTS

I would like to express my sincere gratitude to Dr. Venumadhav Korampally for his continuous support and guidance in this thesis work as well as throughout my graduate study. I also wish to express my appreciation to Dr. Martin Kocanda for his help in successful completion of my thesis. I would also express my sincere gratitude to Dr. Suma Rajashankar for her continuous support and guidance throughout my graduate study.

I would like to express my gratitude to the thesis committee members, Dr. Michael J. Haji-Sheikh and Dr. Donald S. Zinger, and the Department of Electrical Engineering for providing necessary equipment and material which led to successful completion of thesis.

I would like to thank my father, Srinivas; my mother, Latha; and sister, Vinewwhi, for their unconditional love, continuous support, enduring patience and inspiring words.

Finally, I would like to thank my friends and everyone who has directly or indirectly helped me for the cooperation.

TABLE OF CONTENTS

LIST OF FIGURES

Page

LIST OF TABLES

Page

Chapter-1

INTRODUCTION

Sensors are being important components in a variety of applications, right from science and engineering to automobiles to electronic devices used in our daily life. The ever - present need for the sensors is driving us to fabricate compact and low-cost sensors. Instrument Society of America defines a sensor as a device which senses physical change in the environment and gives an output response to the specified measurand (input). The output may be optical, electrical, chemical or even mechanical response. Depending on the specified measurand (input), sensors can be broadly classified into chemical, biological or physical sensors (Dorf, 2006); Figure 1). Chemical sensors are the sensors whose measurands are chemical components, namely ion concentration, gas concentrations, humidity, etc. Biological sensor measurands are biological compounds like detecting cancer cells, proteins, antibodies and enzymes. Similarly, physical sensor measurands would be temperature, pressure, optical radiation, velocity, sound, electromagnetic fields, etc.

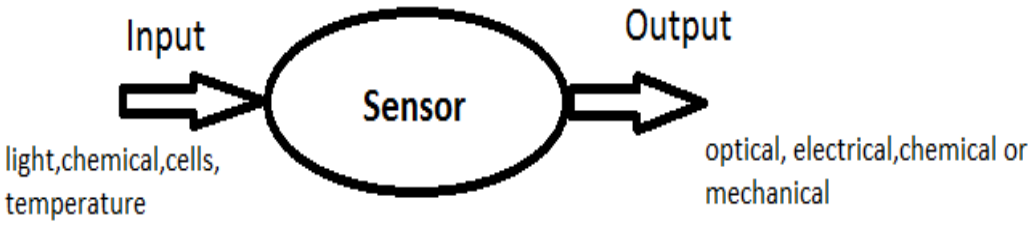

Figure 1 Representation of a sensor

In our thesis we are dealing with the chemical sensors with input of various chemical analytes giving an electrical signal as an output. The main objective of this thesis is to output signal to determine and analyze the sensor response to differentiate between the analytes that are used as the input. Recent work done using the anodized aluminum oxides (AAO) showed that the sensor adsorbs alcohols and cyclic volatile compounds and the response of the sensor measured using impedance spectroscopy showed a unique trend. A similar work is done using nanoporous organosilicate (NPO) sensors and the response obtained through impedance spectroscopy showed a very similar response as that of the AAO. It showed that the response of the NPO sensor exposed to vapors of various chemical compounds had direct relation with the relative permittivities of that particular analyte.

The development of the chemical sensors responds to the chemical data that needs to be characterized whether may it be in form of human bodies, measuring quality of the natural air, or even for the control of industrial toxins. Due to the increasing need in all these aspects, demand in manufacturing of chemical sensors is rising. The main advantage of chemical sensors is portability, small size and cost effectiveness (Banica, 2012). However, these chemical sensors are much needed to detect even the smallest change in the measurand; thus the challenge of attaining more

sensitivity in chemical sensitivity and fabrication of such devices is necessary. In this challenge to develop more sensitive chemical sensors the most important trend is nanotechnology.

1.1 CHEMICAL SENSOR

In definition a chemical sensor is a device that could provide a real-time output response about a test sample. In general a chemical sensor performs two operations: recognition of the analyte and transducing its response into an analytical response. So, when an analyte approaches the sensing element (the electrodes) some of the physical or chemical parameters of this sensing element vary and it sends this change as a response to an external environment for the analysis purposes. A chemical sensor can be used in many purposes like detection of enzymes, recognition of biological cells, recognition of nucleic acids, etc. However, in recent studies many advancements are made in detection of gases and vapors. General recognition methods include the process of adsorption at the surface or absorption by the sensor material. Depending on the target material the sensor is chosen, like metals, polymer materials or inorganic compounds. The chemical sensors are now mainly used in the detection of harmful gases and some of the gases in industries.

1.1.1 HISTORY OF CHEMICAL SENSOR IN NANOTECHNOLOGY

Chemical sensors were used from the nineteenth century. However, previously there used to be complex chemical sensors like the gas chromatography and ion-mobility spectroscope for detection of various chemical analytes and in discriminating between various chemical compounds (Figure 2). The canary is a hand - held air quality measuring device that was used by miners to

detect the presence of harmful and fatal gases like carbon monoxide. These were not only complex but also expensive and hence cannot be used for commercial purposes. As time is advancing chemical sensors were required in low-end sensing purposes like for air quality measurement in houses, breath analysis, etc.

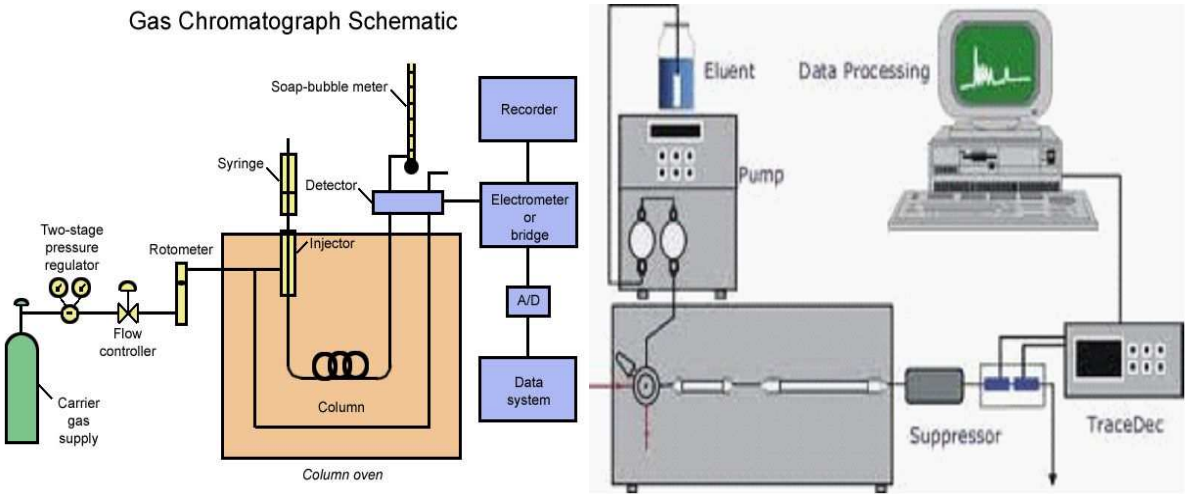

Figure 2 a) Gas chromatograph (WOHLworks) b) Ion mobility chromatography (Morsi, 2013)

So to make these chemical sensors accessible to the low-end usage purposes a new-approach needs to be adopted. As a result of this, miniaturization of the sensors was required. Here came the concept of microelectronic sensor in 1970s. This was fabricated for low-cost and user-friendly but the disadvantages of include non-reproducibility, stability and sensitivity. Hence further work was done which thus resulted in thin-film sensor.

The thin film could solve the problem of reproducibility but couldn't discriminate between the analytes in a single sensor, hence resulting in an array of microelectronic chemical sensors. The description of overall history of chemical sensor is beyond description of this thesis; however, after continuous efforts being made in the field of chemical sensors, porous silicon was used as a

sensing element. Here came the concept of porous materials. After porous silicon, now nanoporous anodized aluminum oxide (AAO) is being widely used as a chemical sensor due to its repeatability, stability and sensitivity. The main advantage of this nanoporous AAO is controllability of the pore dimensions. Under this issue lies the concept of nanotechnology.

1.2 NANOTECHNOLOGY

Nanotechnology is the branch of science which deals with particles at the scale of 1 billionth (10^9) of a meter; it is also the study of manipulating matter at the atomic and molecular scale. Nanoparticle is the fundamental component used to fabricate nanostructures. The size of nanoparticles ranges between 1 and 100nm and have different physical and chemical properties when compared to bulk metals, like lower melting points, higher surface areas, optical properties, mechanical strengths, etc.

1.3 NANOPOROUS SENSORS

Porous materials with small pore sizes and large surface areas are indispensable in the industrial, scientific and also domestic purposes. Over past decades many advancements are made in the sensor technologies using these nanoporous materials in the fabrication of the sensors. Nanoporous materials are ideal in fabricating sensors with high sensitivity because using these materials not only increases the thermal and mechanical strength but also increases the analyte surface interaction due to its large surface areas, thus leading it to even achieve low detection limit of the analyte. Thus a large experimentation on using these nanoporous materials in gas detection

is being made. In addition to the use of the nanoparticles in gas sensing, numerous advancements were made in the field of science and engineering using these nanoporous materials.

The porous nature of the oxide films were first exploited in 1950's after the invention of the electron microscope. Keller et.al (1953) described that the porous structures contained uniformly spaced hexagonal structures.

Some of the nanoporous sensors used in various fields of sensing include detection of cancer cells, humidity and ammonia gas sensing application, etc. (Kiran Bhattacharyya, 2012) mentioned a method to detect initial cancer cell in the human body. Gold nanoparticles have an interesting property that makes them ideal in detection of cancer cells. This property is to scatter the absorbed light. Many cancer cells exhibit a receptor (EGFR) all over their surface. These receptors can be used as targets in detection of cancer cells. By binding the gold nanoparticles to the antibody of EGFR, the nanoparticles target and patch to the cancer cells. Once it is attached to the cancer cell the gold nanoparticle will reflect light when exposure to light, differentiating between healthy cells and the cancer cells. These gold nanoparticles are not only used for the detection of cancer cells but also used for many different purposes, like curing of diseases, detection of proteins, vapor detection, etc. The nanoparticles are not only used in detection of the cancer cells but can also act as drug delivery systems by detecting the cancer cells and directly delivering the medicine to the targeted site.

The porous nature of the oxide films were first exploited in the 1950s after the invention of the electron microscope. Keller et.al(1953) described that the porous structures contained uniformly spaced hexagonal structures. Later work on controlling the pore diameter and interpore spacing on the anodization voltage was done. Later refinements on fabricating ordered porous alumina with defined pore structure was done using different electrolytes, namely malonic acid,

and was demonstrated that use of malonic acid resulted in corrosion resistant characteristics (Lee, 2007). These AAOs are used in numerous applications, mainly for humidity sensing.

Oomman K.Varghese(2002) demonstrated humidity and ammonia sensing using nanoporous alumina films. It also demonstrated the effect of pore size and uniformity on the response of the nanoporous alumina in ammonia and humidity sensing. It was demonstrated that the sensor with smaller pore diameter is sensitive to wide range of humidity values and also showed more sensitivity for ammonia (Oomman K. Varghese, 2002). The study also included the mechanism of conduction through the porous alumina. It said that the alumina senses the presence of the ammonia based upon ionic conduction. Ionic conduction is a mechanism of movement of ions of the analyte from one site to another through the vacancies. This ionic conduction at the surface of the alumina decreases the overall sensor impedance by donating electrons to the conduction band in the base material.

1.4 ANODIZED ALUMINA OXIDE (AAO)

While using ceramics with various metal oxides including alumina, mainly for humidity sensing, experimentation was done with anodized aluminum oxide (AAO) (Martin Kocanda et.al, 2009) in sensing various analytes. It was demonstrated that the AAO showed response to these analytes where the analytes were alcohols and cyclic volatile compounds. Anodized alumina oxides consist of two layers; the below layer is a metal oxide layer and the above layer is a porous layer grown from the oxide layer.

Nanoporous anodized aluminum oxide has gained much importance due to its physical and chemical properties. The pore structure can be controlled by using different electrolytic solutions

for anodizing and thus making it one of the most researched materials in the nano-materials. Firstly, to know what is anodization, anodization is a process to coat a metal with a protective oxide layer by an electrolytic solution. Aluminum is a metal with highly valid properties such as low specific gravity and good mechanical properties. Due to these reasons alumina plays a very important role in many applications. Thus due to these reasons nanoporous AAO was commercially manufactured as a low-cost sensing device for various applications. Recent study of detecting various volatile organic compounds is done using AAO. It proved to be an efficient sensing device in detecting and distinguishing between various chemical analytes. Thus due to these reasons nanoporous AAO was commercially manufactured as a low-cost sensing device for various applications.

Initially it was observed that the aluminum surface subjected to weathering becomes coated with the thin natural oxide film able to passivate and protect the aluminum against corrosion even if that protection was not long lasting. This observation triggered a research process in obtaining an artificial oxide with superior corrosion resistance and stability properties. Thus in 1911 anodizing Al in sulphuric acid solution was discovered.

For the production or fabrication of nanoporous thin film, initially the substrate material is used with the 99% alumina level; it is chosen because of ease for use and low cost of raw material. A smoothing layer (Radzik et. al, 2008) is printed on the alumina surface in order to produce the substrate that should have to be compatible with the deposition of the thin film. Later on for producing robust anodized alumina oxide films an adhesion layer of TiW (because of its high affinity) is produced using sputter deposition technique. Then this TiW layer is exposed to 3% oxalic acid at 40 V for several hours; then using the CVC deposition with rotating anode is used to develop a film with multiple sub-monolayers of alumina. After this step the formed film is

anodized with platinum as cathode and the deposited alumina on the silicon layer as anode. Finally the anodized alumina films are rinsed for 15 min with the deionized water and spin dried. Figure 3 illustrates the pore formation mechanism in an anodizing of aluminum. After the exposure of alumina to the electrolytic solution in presence of current aluminum oxide is formed at the surface of the alumina. Upon constant exposure of this aluminum oxide in the electrolytic solution pore tends to appear on the metal oxide layer.

Now that the alumina film is fabricated, anodized alumina oxide sensor is developed by the screen printing of electrodes. Thus the fabricated anodized alumina oxide films that can be used for sensing of various analytes may be humidity, ammonia, or any organic compounds.

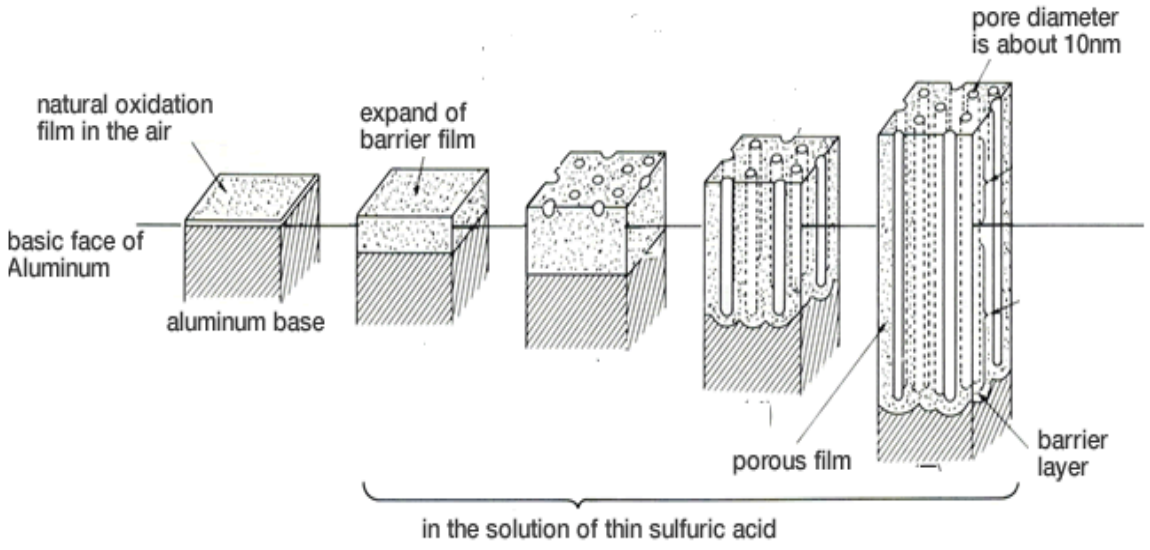

Figure 3 Pore formation mechanism of nanoporous anodized aluminum oxide (NACL)

Other than the anodized alumina, porous silicon also gained much attention. However the fabrication processes of these materials are quite different. Despite the evolution of graphene, gallium with high electrical properties, silica is much preferred substance in the semiconductor

devices and many electronics. This may be because silica is most abundant material on the earth and is cost effective. Porous silica gained much importance due to its quantum effects identified by Ulrich Gösele and V. Lehmann(1991). These porous silicon structures are fabricated by the process of electrochemical etching (Losic, 2015). Mixtures of hydrogen fluoride (HF) and nitric acid (HNO_3) have been widely used. Initially it is required to remove any formation of the oxide layer on the commercially available silicon wafer is important as it may act as contaminants during etching. Immersing the wafer in HF solution may remove all the impurities and make the wafer perfect for the etching. So as the wafer is free from impurities an etching cell must be set up for the etching process. In this process metals like gold and platinum are to be selected as the etching element as they are inert. At this step etching is done by placing the silicon wafer in the test cell and exposing it to HF solution with the platinum immersed inside the HF solution. Thus the fluoride (F^-) ions form bonds with the silicon (Si) thus creating an electron hole on the substrate leading to the formation of porous silicon. The porous silica was used for applications as biosensors, for drug delivery, in optical sensors, etc. Many advancements were made in the fabrication process of the porous silicon and anodized alumina oxides (AAO) in regulating the pore size and thickness of the film. In AAO the anodization potential and the electrolyte amount variation may lead to the formation of well-defined pores. It was demonstrated by Varghese et.al (Oomman K. Varghese, 2002) single-step anodization resulted in more disordered pores whereas double-step anodization process resulted in ordered and smaller pores.

1.5 Nanoporous Organosilicate (NPO) Films

Further on there are many types of synthesis processes like colloidal method, sol-gel, porogen approach and surfactant templating. These methods prove to be competitive due to their

low cost of the precursors, complexity of kinetics, repeatability, and time required for the fabrication (Chitra Agashe, 2008). As any application requires a fast-obtained yield at low cost with no compromise on the sensor characteristics, nanoparticle-polymer composites were considered. These nanoparticle-polymer composites have advantages in optical, electrical and mechanical properties (Anna C. Balazs, 2006). It was demonstrated that the nanoparticles could be self-assembled due to the collision nature of the ligands on the nanoparticle surfaces. Nanoporous organosilicate (NPO) films are based upon this concept of nanoparticle-polymer composites. As fast-integrating circuits are necessary for the faster sensing, low dielectric (*k)* constant films are to be used instead of the metal oxide devices. Among many materials that are tried in replacing these metal oxides, PMSSQ is one of the most widely researched materials because of its compatibility in fabrication of the film, thermal stability and its hydrophobic nature. It was stated that PMSSQ has a dielectric constant of 2.6-2.8 which could be further reduced upon decreasing its density (Hyeon-Lee, 2005). The density of the PMSSQ can be varied by introducing pores into the PMSSQ nanoparticles, thus reducing the overall nanoporous film. But as the mechanical strength is important for any film to integrate into the electronic devices as a sensing device, these PMSSQ are mixed with a precursor solution. This precursor solution is mainly a polymer that could increase the durability and mechanical strength to the film. One of the main advantages of the PMSSQ-based films is the hydrophobicity. The metal oxides have a tendency to adsorb moisture from the atmosphere and thus degrade in their performance, whereas the PMSSQ based films being naturally hydrophobic doesn't have the capability to adsorb moisture, thus increasing the efficiency.

1.6 Preparation of NPO

The material extensively used for the nanoporous organosilicate films deposition contains the polymethyl silsesquioxane (PMSSQ), polypropylene glycol (PPG), propylene glycol methyl ether acetate (PGMEA). As PMSSQ is hydrophobic, these PMSSQ molecules are bound together by PPG forming a network-like structure during the porous film formation. The basic methodology of pore formation here is the porogen approach where a pore generator (porogen) is chosen such that evaporation of this porogen results in the formation of porous NPO.

The nanoporous film was prepared using a heat decomposition method to produce films from suspensions of polymethyl silsesquioxane (PMSSQ; Techneglas) nanoparticles in polypropylene glycol (PPG; m.w. 425), which was dissolved in propylene glycol methyl ether acetate (PGMEA) (Korampally, 2009). This method allows for the control of the film porosity and film thickness by controlling the by-weight concentrations of PMSSQ and PPG in the precursor solutions and by controlling the temperature used for decomposition.

NPO films used for the work discussed in this chapter were a 5555 solution, which had a 5:5 weight ratio of solvent (PMA) to solute (PPG and PMSSQ), where the solute had a 5:5 weight ratio of PPG to PMSSQ. All films were spin coated onto the silicon wafer substrates at 3000rpm/30sec and then decomposed by placing the coated wafers on a hotplate at 500°C/5min (Figure 4). During this decomposition process, due to the heat the PMSSQ nanoparticles attain Brownian motion and are self-assembled crosslinking with other PMSSQ molecules to form porous film. Wafers were then air cooled to room temperature.

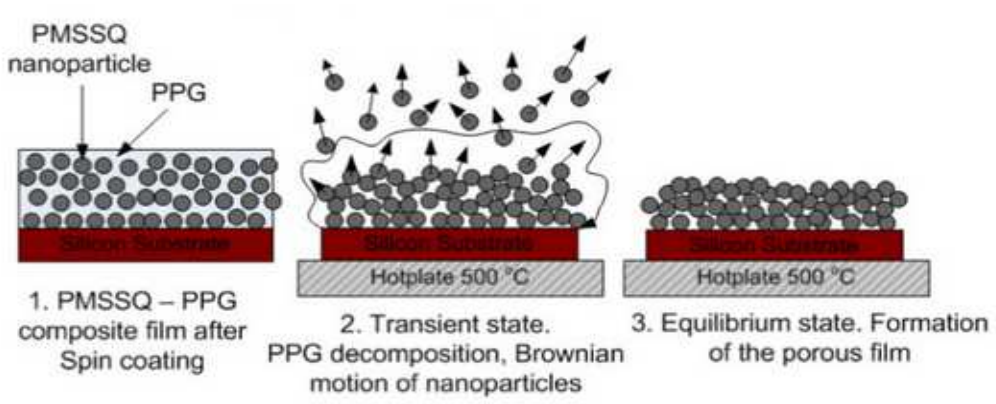

Figure 4 Schematic of Formation of NPO film formation (Korampally, 2009*)*

The PMSSQ molecules in the solution of PPG and PMSSQ are bound together by PPG. PPG contains the hydroxyl groups leading for the crosslinking of the matrix of PMSSQ molecules, with the PMSSQ attaining globular structure. PPG acts as a medium between PMSSQ molecules as the PMSSQ are hydrophobic. Upon exposure of the spin-coated films to a preheated hotplate at 500°C, the PMSSQ nanoparticles attain Brownian motion and interparticle collisions occur. During these collisions some of the PMSSQ molecules attain greater kinetic energy and are evaporated from the spin-coated film. At this step the decomposition of PPG occurs at low temperatures of ≈200ºC. Thus the PMSSQ molecules crosslink among themselves, no longer using PPG for the interconnection. The remaining PMSSQ nanoparticles on the film align themselves, attaining stability after the decomposition, forming a nanoporous film. However, the pore diameter is dependent on the weigh ratios of the PPG and PMSSQ in the solutions. Figures 5 and 6 show the cross sectional view of the formed NPO film at magnifications of 1µm and 100 nm.

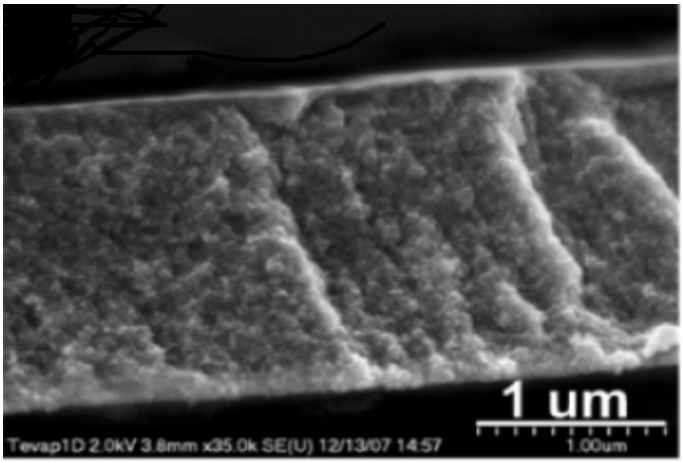

Figure 5 SEM image of the cross sectional view of NPO 1 μm magnification

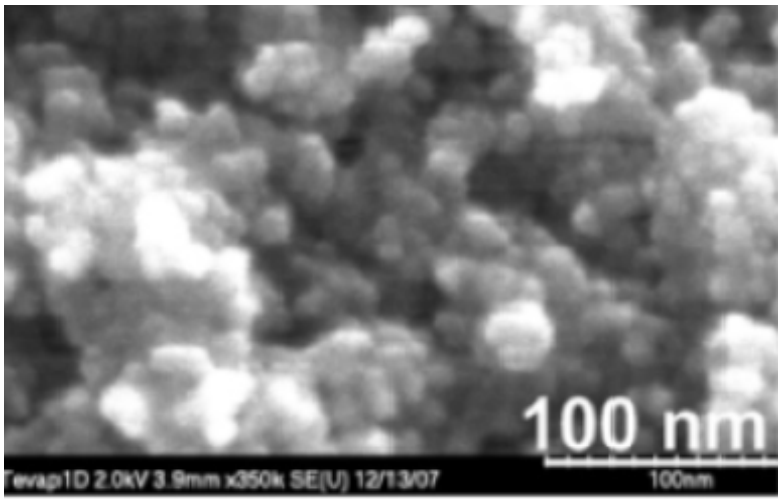

Figure 6 SEM image of the cross sectional view of NPO 100 nm magnification

The conduction mechanism in the nanoporous organosilicate sensor within the subtract size of about 10nm was extensively gaining prominence related to offering two distinct benefits over

the planner material that is related to integrating the scheme of sensing that has the following characteristics:

1. Broad surface area
2. Capillary condensation

Capillary condensation is a process of condensation of vapour at the porous membrane. The vapor condenses at the surface of the porous film (liquid-vapor interface) due to the Van der Waal's forces acting between the substrate and the vapor. After this condensation, the liquid adsorbed onto the surface of the NPO increases the overall sensor conductance increase, leading to the change in the sensor response.

1.7 Impedimetric Sensing

The sensor response is always measured in terms of real and imaginary impedances, namely Nyquist plot. These plots are plotted with real impedance on x-axis and imaginary impedance on y-axis. Thus to measure a response of a sensor, measuring impedance is necessary. This measurement of impedance for analyzing a sensor response is called impedimetric sensing and measured using impedance spectroscopy.

1.7.1 Impedance Spectroscopy

The impedance spectroscopy contains the source of the variable programmable frequency that provides the ability for the generation of a sinusoidal alternating current waveform with the adequate amplitude level to efficiently excite the sensors (GamryInstruments).

Over the past two decades, electrochemical impedance spectroscopy (EIS) has emerged as the most powerful of electrochemical techniques for defining reaction mechanisms; however, most of the work was done in analyzing the system response in liquid-electrode interface. The impedance spectroscopy came into theory in 1894 with the application of Wheatstone bridge by Nernst for calibration of dielectric constant for different electrolytes (The Electric World, 1987). This approach was later implemented to calculate dielectric constants of the galvanic cells, diffusion mechanism, etc. In 1920 it was implemented on biological systems and it was observed that there is relation between the frequency component of impedance and constant phase angle. Later on two brothers, Cole and Cole, suggested that this relation is in the form of a depressed semicircle (Licker, 2005). From then the impedance spectroscopy was used in the field of electrolytes, chemical solutions, rotating disks and many other fields for the analysis of the system response based on the Cole-Cole plot. The impedance spectroscopy has wide range of applications which cannot be mentioned in detail.

1.7.2 Working Principle of Impedance Spectroscopy

The basic working of the impedance spectroscopy relies on a Wheatstone bridge (MarkE.Orazem, 2011). This bridge is used to measure the impedance of the measurand by adjusting resistor and capacitor at each frequency. A signal generator generates a sinusoidal signal based upon the input parameters and is applied to the sensor, thus obtaining the sensor response in terms of real impedance and imaginary impedance. In earlier stages different components are used for these operations but as of now all of them are embedded into a single system. The obtained

sensor response is represented as Nyquist plots or Cole-Cole plots with the real impedance on x-axis and imaginary impedance on y-axis respectively.

Figure 7 shows a typical representation of the Nyquist plot of a parallel RC network. However, practically a perfect semicircle is not obtained. It represents the real impedance on x-axis and imaginary impedance on y-axis. ω is the frequency with lowest frequency on the right and highest frequency on the left.

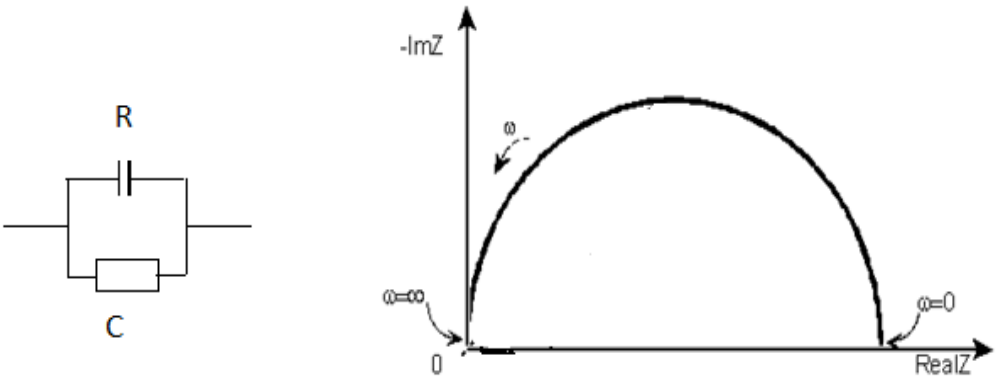

Figure 7 Typical representation of a Nyquist plot of a parallel RC network

Electrochemical impedance spectroscopy is a useful tool when a number of analyses are to be done using a single response.

1.7.3 Advantages and Disadvantages of EIS:

Advantages of EIS include:

- Time optimization
- Less apparatus

- Both time domain and frequency domain analysis can be done at the same time
- Portability
- A very low frequency analysis can also be done varying from 100Hz.

Disadvantage of EIS is the high cost of the equipment.

EIS is mostly used in fast-changing environments like in nanoporous materials where the response of the substrate is observed within a few seconds of the exposure to the analyte. Thus in these cases EIS can even record very minute response at intervals of 0.1 sec. Hence this is the most widely used tool to analyze a sensor response mainly in gas sensors. Recent work in nanoporous sensors done by G. Martin Kocanda et.al (2009) using an EIS showed a trend in the response of the AAO when exposed to various alcohols, cyclic volatiles and water. In our thesis a similar experiment is being done using EIS for the analysis of NPO sensors on exposure to various analytes.

Chapter-2

EXPERIMENTAL

The fabrication of NPO sensor is made at Northern Illinois University by Dr.Venumadhav Korampally. It entails PMSSQ nanoparticle formation, NPO films (from PMSSQ nanoparticle solution) and screen printing of electrodes onto NPO films.

2.1 Preparation of PMSSQ Nanoparticle Solution

PMSSQ nanoparticle solution is prepared by mixing of two solutions. Solution 1 is a mixture of PMA (solvent) and PPG (solute); solution 2 is a mixture of PMA (solvent) and PMSSQ (solute). However the amount of solvent and solutes depend upon the specifications of the NPO film you want to fabricate. After preparation of solution 1 and solution 2, mixing both the solutions together by the desired weight ratio initiates polymer collapse due to PPG and thus leading to the formation of PMSSQ nanoparticles. In this thesis we are using 5555 NPO substrates.

2.1.1Preparation of 5555 NPO Substrates

Here initial 5-5 represents the weight ratio of PMA: PPG (solvent 1) and PMA: PMSSQ (solvent 2) and the later 5-5 represents the weight ratio of solvent 1: solvent 2.

2.2 Fabrication of NPO Thin Films

Now as the prepared solution contained the PMSSQ nanoparticles, the solution (with PMSSQ nanoparticles) is spin-coated onto a n-silicon wafer for 30 sec at 3000rpm.

During this spin coating process the PMA is evaporated leading to the formation of uniformly coated films. These films are then subjected to a hotplate at 500ºC to stabilize the nanoparticles and forming a hydrophobic porous NPO film. The pore formation mechanism is discussed in Section 1.6. For the fabrication of a nanoporous organosilicate (NPO) sensor, the obtained NPO film is screen-printed with Pd-Ag interdigitated conductors on the surface. The sensors are then cut from the wafer and are sequentially numbered as 1, 2...12 for further experimental purposes as in Figure 8.

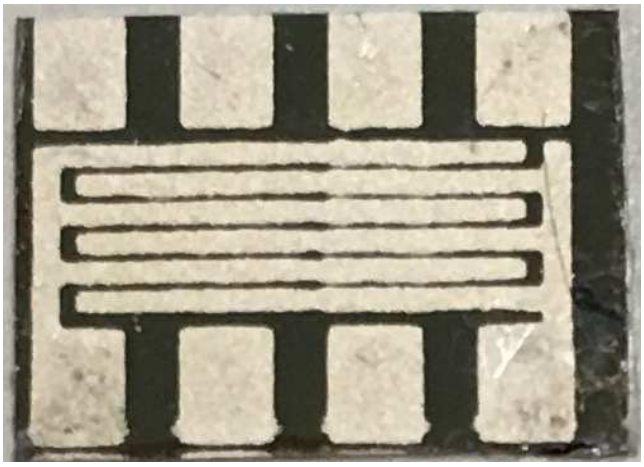

Figure 8 NPO sensor after screen printing of electrode

2.3 Sensing Setup

The set-up used for the sensing of the NPO sensor for vapors of organic solvents is shown in Figure 9. The figure typically represents a block diagram of a sensing setup specifying how Ivium compactstat acts as an interface between the NPO sensor and the computer.

Figure 9 Block diagram representation of the sensing setup bench for response of the NPO sensor to different analytes

Ivium Compactstat is an electrochemical interface and impedance analyzer purchased from Ivium Technologies. This is controlled by Ivium Soft which is a predefined software controlling the instrument functions, analysis and data management. The instrument can be operated via USB port from a PC and via a probe with electrode clips to the sensor. Figure 10 a shows a Ivium Compactstat connected with USB cable and a probe with the alligator clips for establishing a connection between NPO sensor and electronic instrument for recording the sensor response on the test bench.

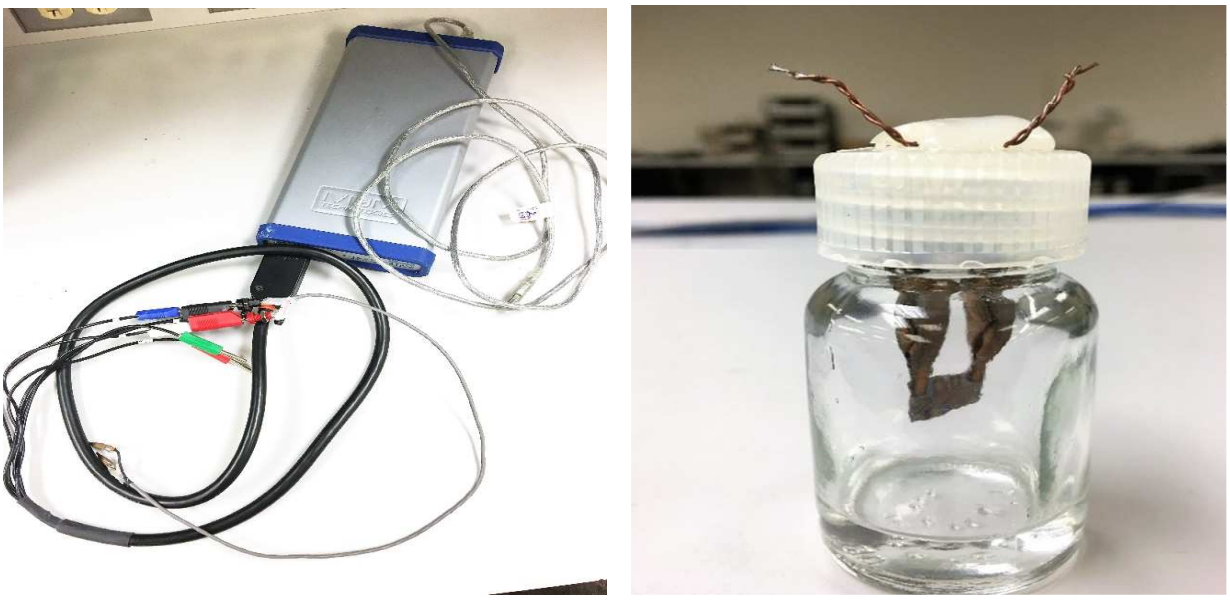

Figure 10 a) Ivium Compactstat, an electrochemical interface between the NPO sensor and the computer b) Glass vial in which the NPO sensor is placed with the liquid analyte whose response is to be obtained

Figure 10 b shows a glass vial, where the cap of the glass vial is soldered with alligator clips to hold the sensor above the vapor - phase analyte. The electrode clippers have copper wires protruding out of the cap of the glass vial for connection between the vial and the Compactstat. The analyte is filled inside the glass vial making sure that the sensor exposed to the solvent is not in physical contact with the liquid analyte.

The glass vial is then connected to the Compactstat via a probe with clippers through the copper wires protruding out of the glass vial; thus making contact between sensor and Compactstat. The Compactstat is connected to the computer using USB cable.

Figure 11 is the diagrammatic representation of the series of steps followed beginning from the process of fabrication of the NPO sensor to the analysis of the response of NPO in different analytes.

2.4 SENSING NPO SENSOR FOR VARIOUS VAPOR - PHASE ANALYTES

The complete thesis is done entailing two stages of NPO sensor:

1. Hydrophobic NPO sensor
2. Hydrophilic NPO sensor

The initially fabricated NPO sensor, i.e. just after the screen printing of electrodes, is hydrophobic (as the PMSSQ films are naturally hydrophobic). Subsequently, this hydrophobic sensor is plasma – treated and the hydrophobic NPO sensor is hydrophilic. In this thesis we could also draw a conclusion between the responses of both hydrophobic NPO and hydrophilic NPO.

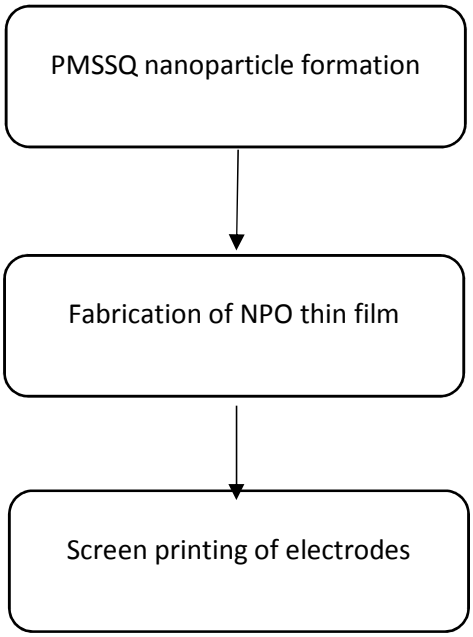

Figure 11 Block Diagram of series of steps involved in the process of the total experiment.
Continued on following page.

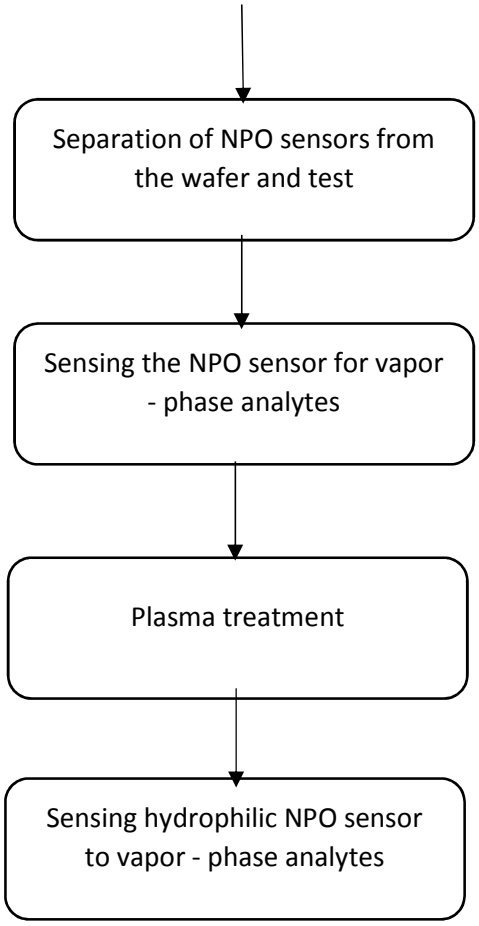

Figure 11 continued.

The response in time domain with both real (resistance) and imaginary (capacitance) impedances is electronically measured when the sensor is exposed to vapors of different organic solvents, namely isopropanol, methanol, n-heptane and deionized water at different frequencies with an amplitude of 100 mV (p-p) sinusoid.

Here I have taken three frequencies into consideration (500 Hz, 1 KHz and 10 KHz). So the responses of the NPO sensor in each of the organic solvent vapors is obtained by varying the above-mentioned frequencies. Subsequently a Nyquist plot is obtained with the respective vapor-

phase analyte by running a frequency sweep from 100 Hz to 100 KHz at 100 mV (p-p) sinusoid. After the experiment is done for the hydrophobic NPO sensor, now the hydrophobic sensor is plasma - treated to get a hydrophilic sensor.

2.5 PLASMA TREATMENT

Plasma treatment is fundamentally a process of inducing charged ions and electrons with high energy due to which it changes the surface properties of the surface that is subjected to the plasma. After plasma treating the surface, impurities are removed and its surface tension increases resulting in a surface that has more tendency to adsorb molecules onto its surface. This plasma treatment can be done based on your requirements by varying the parameters like gas used in the plasma, amount of time, pressure, etc.

In our case we are using a Carbondioxide (CO_2) plasma treatment in low setting for 30 sec, 2.5 flow rate at a pressure of 429 mtorr. Now that our NPO is plasma - treated with the above-mentioned setting, all the impurities from the NPO surface are removed; hydrophobic NPO sensor is now a hydrophilic NPO which should adsorb the vapor-phase analyte with more ease. The response of the plasma-treated NPO is obtained in the same way for the hydrophobic NPO in time domain for real (resistance) and imaginary (capacitance) impedances over frequencies of 500 Hz, 1 KHz and 10 KHz respectively for each of the organic solvents (isopropanol, methanol, n-heptane and deionized water). A comparison of both the stages (hydrophobic and hydrophilic) of NPO can be made depending on the real impedance response in time domain (Figure 12).

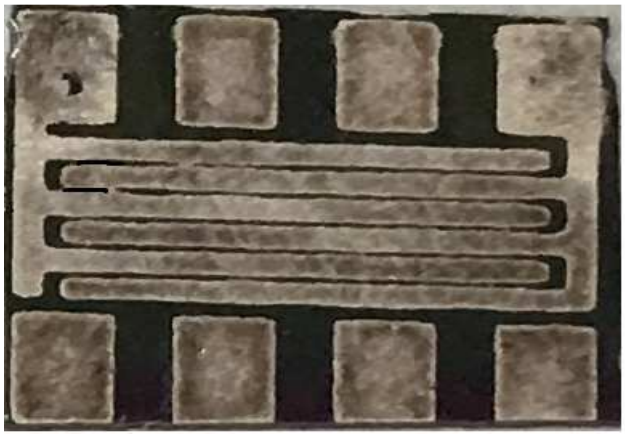

Figure 12 NPO sensor after plasma treatment

Chapter-3

RESULTS AND DISCUSSION

3.1 Preliminary Testing

The sensors obtained after the screen printing of Pd-Ag electrodes were characterized for their performance and are assigned sequential numbers (1, 2, 3 . . 12). The initial resistance (real impedance) and capacitance (imaginary impedance) values of each of the sensors were taken electronically using the compactstat applying 100mV (p-p) sinusoid at 1 KHz. The results are stored in Microsoft Excel format for further use. It was detected that three of the sensors showed no response, due to shorting of the electrodes. The highest capacitance value measured was 320 pF and resistance value was 0.17 MΩ. Figure 13 represents the value of Z_{real}/Z_{imag} to the sensor number. The sensor exhibiting highest Z_{real}/Z_{imag} was taken for the sensing of vapor - phase analytes, as they were proved to have more tendency to discriminate the adsorbed vapor - phase analytes.

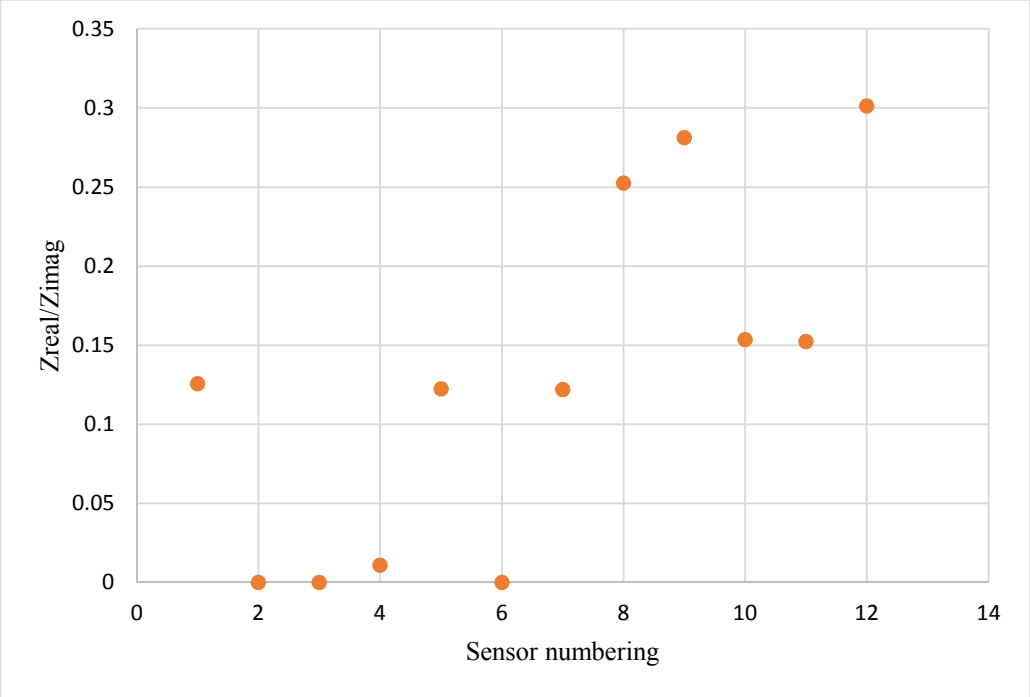

Figure 13 Characterization of the fabricated sensors

As indicated in Figure 13, sensor 8 has greater Z_{real}/Z_{imag} and was chosen for the experiment. (As you notice, sensor 12 and sensor 9 have greater Z_{real}/Z_{imag} but we have already used both of the sensors for some preliminary testing) Sensors 2, 3 and 6 exhibit zero response whereas sensor 4 exhibited very poor response, making them debilitated.

The analytes that were selected are isopropanol, methanol, deionized water (DI) and n-heptane; air was considered as a baseline for the whole experiment. These analytes are chosen with variation from organic compound (n-heptane), polar compound (DI water) and alcohols (methanol, isopropanol). Impedance spectroscopy (Section 1.7) is the analysis method used in our study to obtain response of NPO sensor for different analytes. Similar experiments we conducted on AAO (Martin Kocanda et.al, 2009) sensors and was depicted that the response relies on the relative

permittivity of the analytes used. In our study we expose NPO sensor to organic compounds to determinate if they respond the same way.

3.2 Response of Hydrophobic NPO Sensor

Initially after choosing a sensor with high Z_{real}/Z_{imag}, this sensor is now adjusted to the sensing setup (glass vial) with the liquid analyte inside the glass vial to a level such that the sensor is not immersed into the liquid, ensuring good head space. Each sensor is now subjected to frequencies of 500 Hz, 1 KHz and 10 KHz sequentially for every analyte used (isopropanol, methanol, DI water and n-heptane). The typical real impedance (resistance) and imaginary impedance (capacitance) response in time domain of the NPO sensor when exposed to the vapor - phase analytes will be an exponential curve with decreasing exponential curve for resistance in time domain and vice-versa (increasing exponential curve) for capacitance in time domain. These curves depict that the sensor though hydrophobic shows response to the vapor analytes. Figures 14 to 17 are the typical responses in terms of resistance and capacitance in time domain at 1 KHz. However, the stabilizing time in each of the compounds varies.

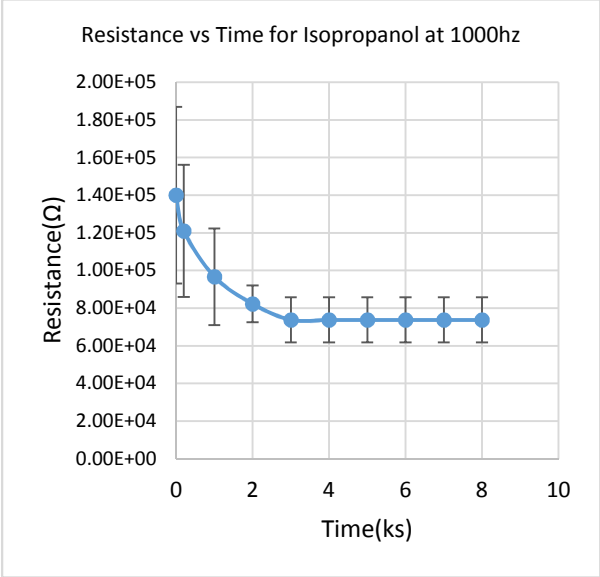

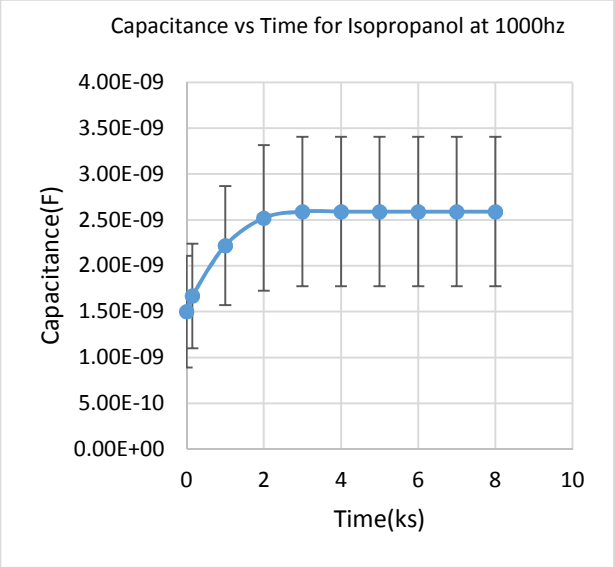

Figure 14 a,b Represents typical response of NPO sensor in isopropanol with resistance and capacitance measured in time domain

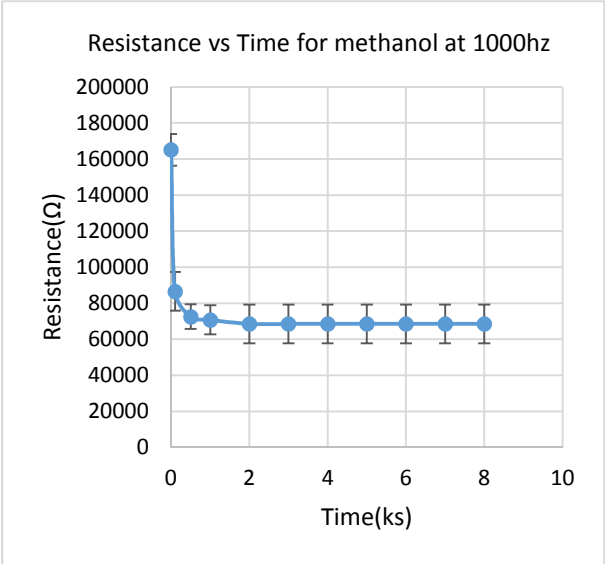

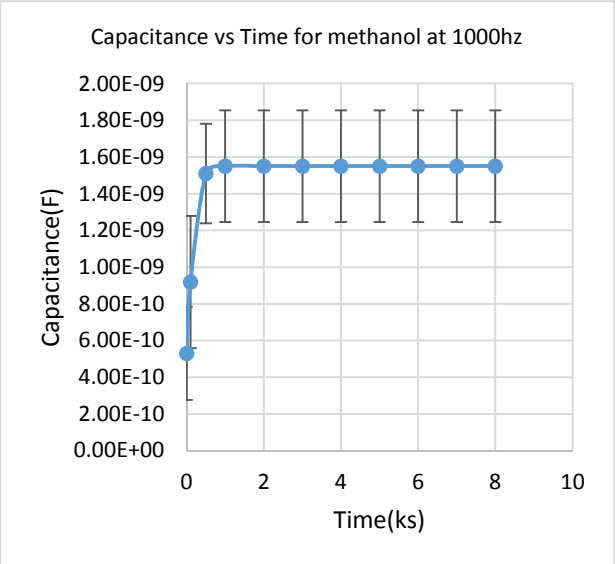

Figure 15 a,b Represents typical response of NPO sensor in methanol with resistance and capacitance measured in time domain

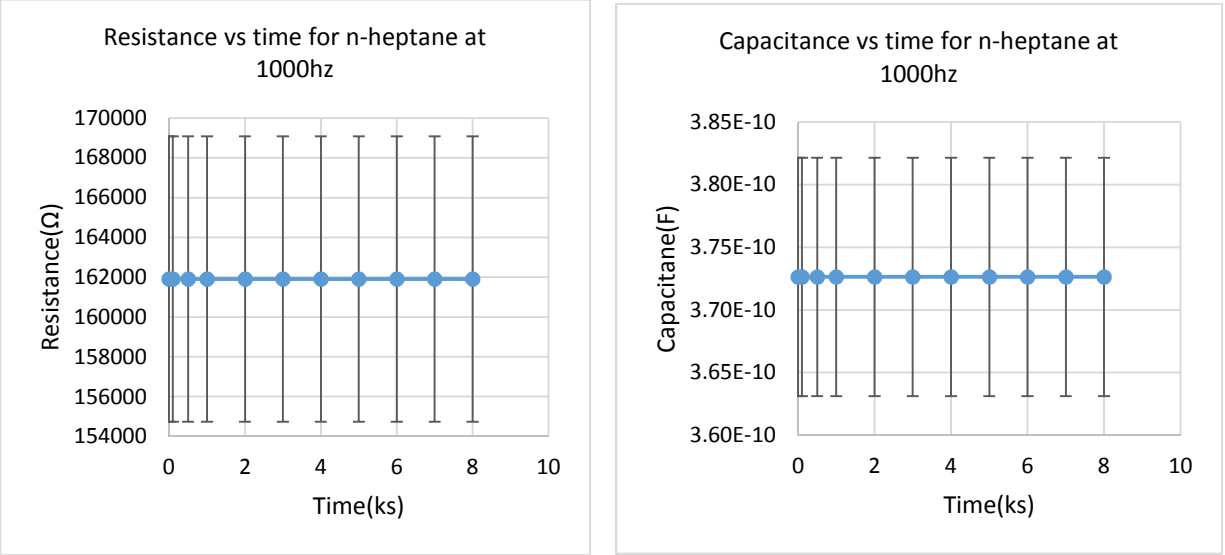

Figure 16a, 16b Represents typical response of NPO sensor in n-heptane with resistance and capacitance measured in time domain

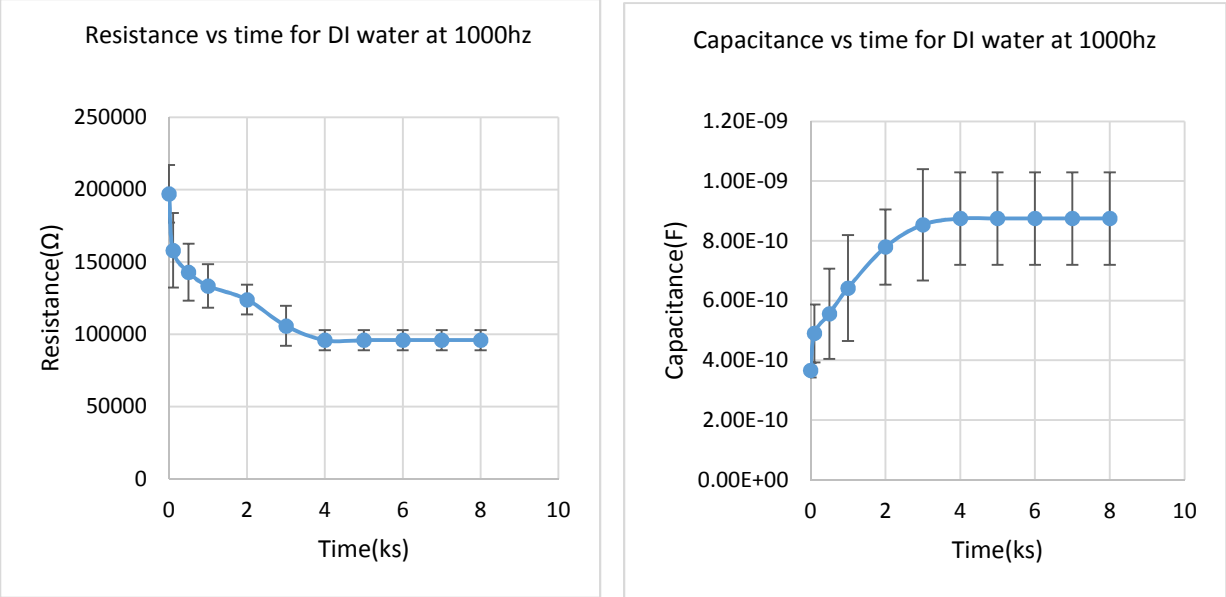

Figure 17a, b Represents typical response of NPO sensor in n-heptane with resistance and capacitance measured in time domain

The measured real impedance and imaginary impedance values are plotted separately with respect to time on x-axis (abscissa) and real or imaginary impedance on y-axis (ordinate). Similar data trend was observed for frequencies 500 Hz and 10 KHz with shift in their initial resistance and capacitance values. Examination of the data indicated that sensor response in methanol achieved stability at ≈630s, faster than in any of the solvents. This may be because methanol is more polar and lighter than isopropanol. Response in methanol (at ≈632s) and isopropanol (at ≈3000s) stabilized faster than the DI water because of the fact that both methanol and propanol are less polar than water due to the presence of non-polar carbon-carbon bond. Though the NPO sensor at this stage is hydrophobic, it showed response to DI water, as water contains H^+ ions and OH^-; H^+ ions are mainly responsible for wetting which may form bonds with the NPO surface by Van der Waal's force. It is also known that the adsorption mechanism in NPO films is mainly due to capillary condensation, where even the polar compounds can be adsorbed leading to the response with DI water as depicted in Figure 16. Important aspect to be noted in Figure 17 is the sensor showed no response when exposed to n-heptane. Initially it was assumed to be very low response that cannot be noticed, but it was proved to be wrong in the latter when the sensor is subjected to frequency sweep from 500 Hz to 10 KHz at 100mV(p-p) sinusoid.

The sensor is subjected to each vapor for three different trials to ensure recurrence. Error bars are plotted taking into consideration these three trials. Standard deviation (SD) at every measured time interval is calculated and error bars are accordingly plotted.

$$\sigma = \sqrt{\frac{\sum_i^N (x_i - \mu)^2}{N}}$$

Where σ = Standard deviation, μ = mean of all the values, x= individual value in the data set, N = total number of values in the data set

Figures 18 represents the measured resistance for frequencies of 500 Hz, 1 KHz and 10 KHz at 100 mV (p-p) sinusoid. It could be demonstrated that the real impedance (resistance) value decreases continuing onto higher frequencies comparatively with high impedance values at lower frequencies. This could be used to indicate the operating range of the NPO sensor, making it more operational at lower frequencies. In Figure 18 as the frequency approached 10 KHz, the resistance value is ≈0.

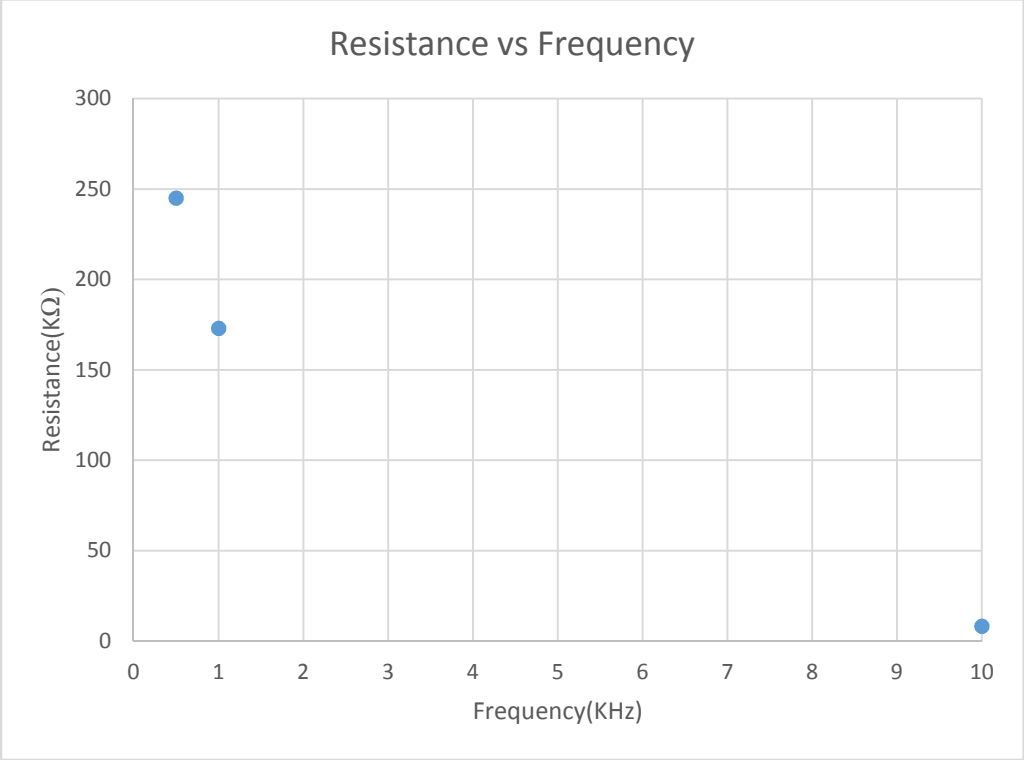

Figure 18 Comparison of the real impedance value of NPO at various frequencies

For the analysis of the adsorption of the analytes onto NPO substrates, a subsequent Nyquist plot or Cole-Cole plot is obtained by a frequency sweep of 100 Hz to 10 KHz with 31 intermediate points at which the real and imaginary impedance values are electronically recorded. The frequency sweep is performed upon stabilization of the NPO in each analyte. Figure 19 represents a Nyquist plot of the hydrophobic NPO sensor with respect to vapor - phase analytes. It is noticeable that the response in n-heptane coincides with the response of NPO in air (baseline), indicating that the NPO irresponsive to n-heptane may be due to very high vapor pressure, thus remaining in vapor - phase even after getting adsorbed onto the NPO, and also may be because of the lacking free H^+ ions which are mainly responsible for wetting. The hypothesis of not much distinction is observed among the analytes considered for the experiment because the NPO film is

hydrophobic. Further work was required to analyze the impedance spectroscopy responses of the same analytes if the NPO was hydrophilic. For this purpose, as an advancement to the initially fabricated NPO sensor, the NPO is exposed to mild CO_2 plasma (as mentioned in Section 2.5) for 45sec at 429 mTorr. Now that the NPO substrate is plasma treated, the surface of the NPO is hydrophilic.

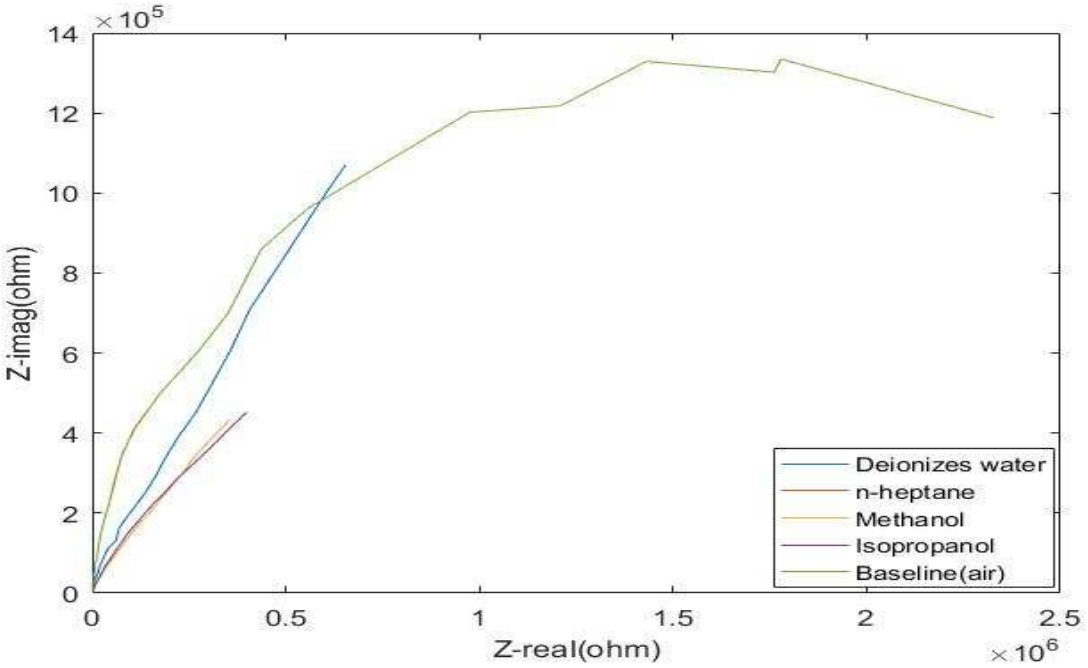

Figure 19 Nyquist plot showing frequency response of hydrophobic NPO sensor in methanol, isopropanol, n-heptane, DI water and air (baseline)

3.3 Response of the Hydrophilic NPO

The same set of experiments as is done with the hydrophobic NPO is done with the plasma-treated NPO (hydrophilic) and compared. It was observed that the analytes showed better response with the plasma - treated NPO. The plasma - treated NPO is placed in the test cell (glass vial) and connected to the external sensing setup. For each of the analyte taken, resistance and capacitance

values are electronically recorded and used for further analysis. All of the experiment is done at a setting of 100 mV (p-p) sinusoid for a time period of 8000 sec (until the response is unconditionally stabilized). Again considering three frequencies (500 Hz, 1 KHz and 10 KHz), graphs were obtained for the tabulated resistance and capacitance of the plasma - treated NPO sensor.

The Figure 20 represents the resistance value of the NPO sensor (plasma - treated) with frequencies of 500 Hz, 1 KHz and 10 KHz. When compared with Figure 18 the resistance at all the frequencies is more than double, thus supporting better sensing characteristics of the hydrophilic NPO sensor (because higher resistance implies higher resistivity to the flow of charge).

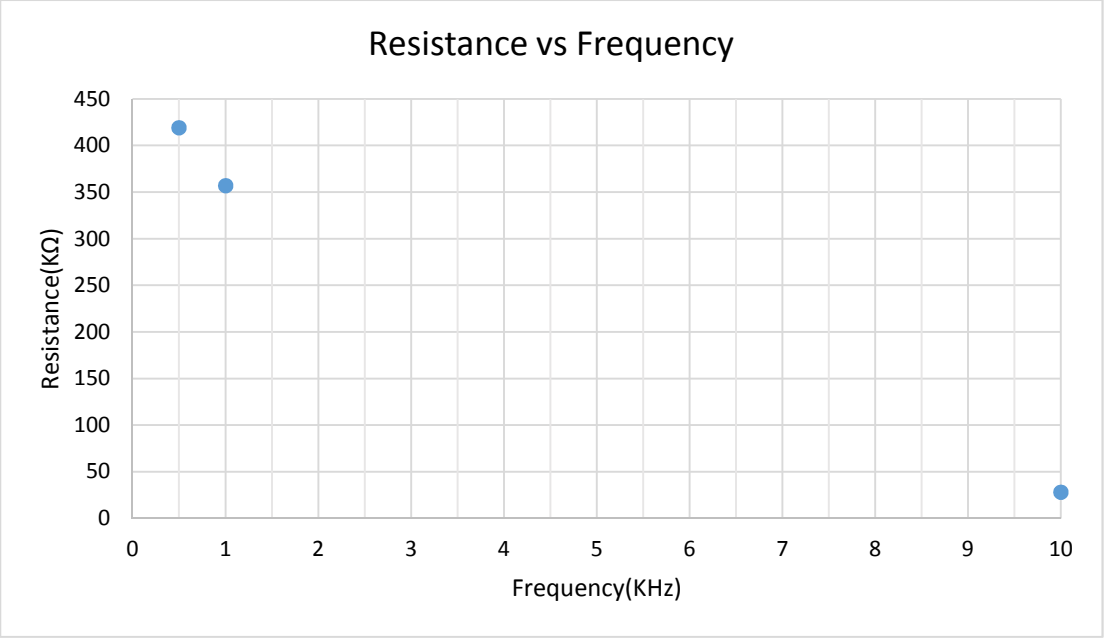

Figure 20 Representation of the plasma - treated NPO response in air at frequencies of 500 Hz, 1 KHz and 10 KHz in terms of resistance

Figures 21 to 24 represent the response of the NPO sensor after plasma treatment in different analytes. It is evident that the sensor is responsive to every analyte irrespective of the level of sensitivity. This supports that the hydrophilic NPO sensor can be used in sensing various analytes. These responses show comparatively smaller error bars than that of the hydrophobic NPO sensor responses in Section 3.2, supporting more recurrence at this stage. Error bars are obtained as mentioned in the Section 3.2 by taking the standard deviation (SD) and the response plotted with the mean of all the three trials. A Nyquist plot or Cole-Cole plot is obtained by subjecting the NPO sensor to various analytes. It is made sure that the response is electronically recorded after the sensor is stabilized.

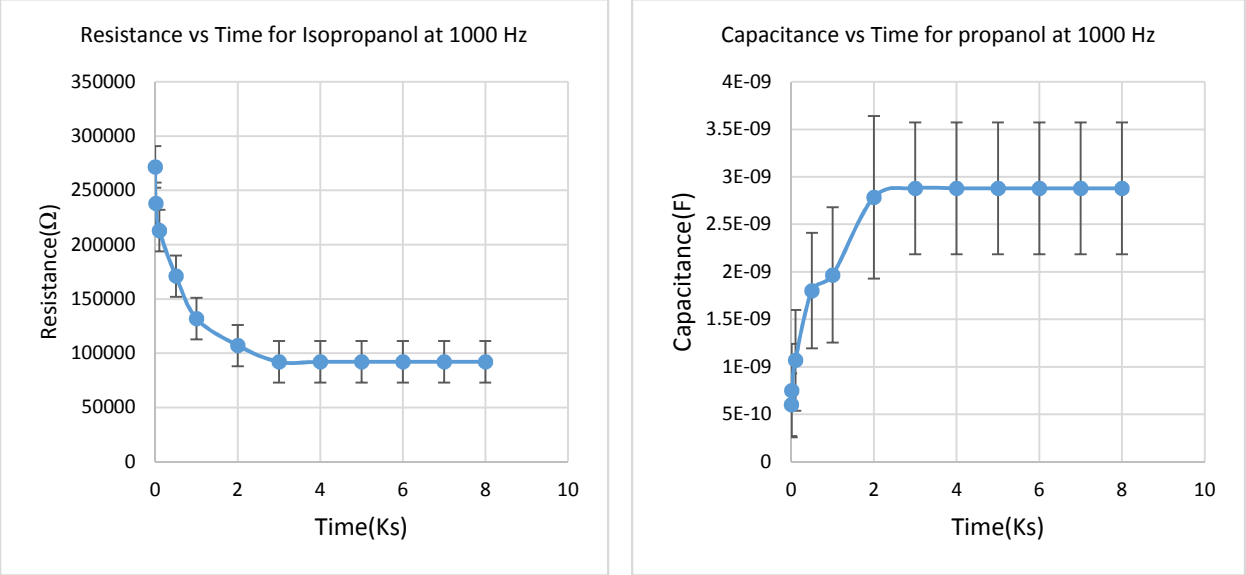

Figure 21a,b Represents typical response of hydrophilic NPO sensor in isopropanol with resistance and capacitance measured in time domain

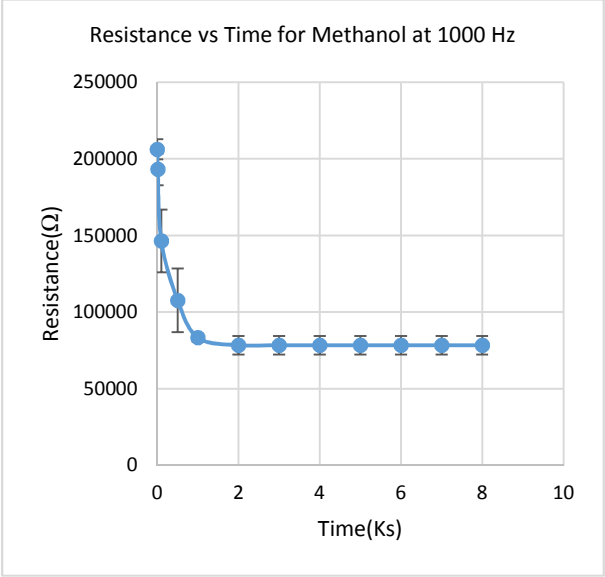

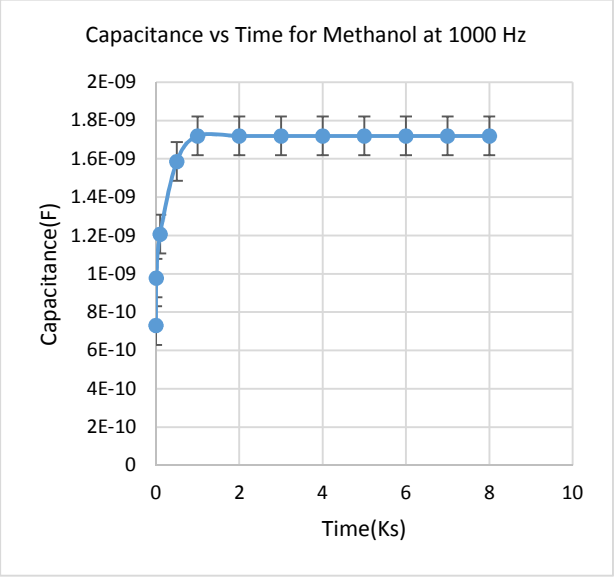

Figure 22 a, b Represents typical response of hydrophilic NPO sensor in methanol with resistance and capacitance measured in time domain

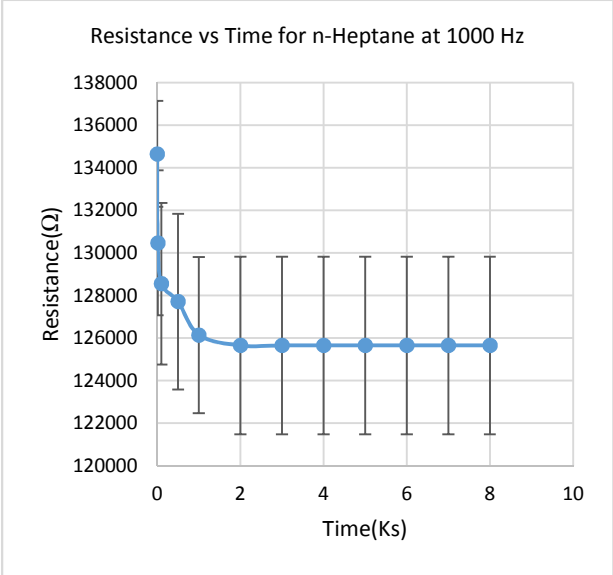

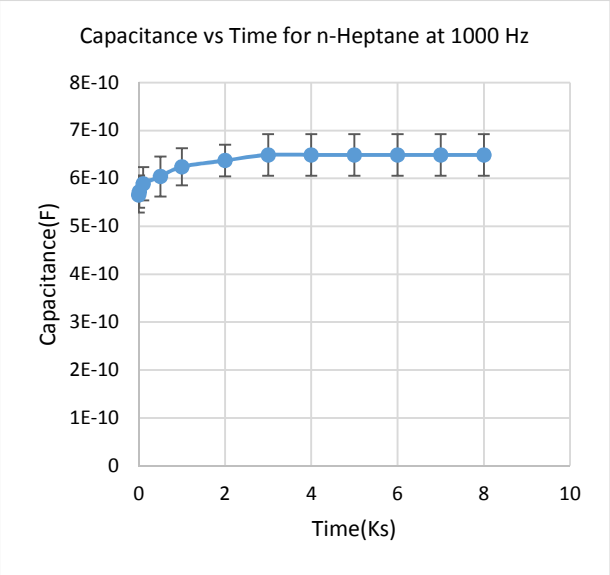

Figure 23 a,b Represents typical response of hydrophilic NPO sensor in n-heptane with resistance and capacitance measured in time domain

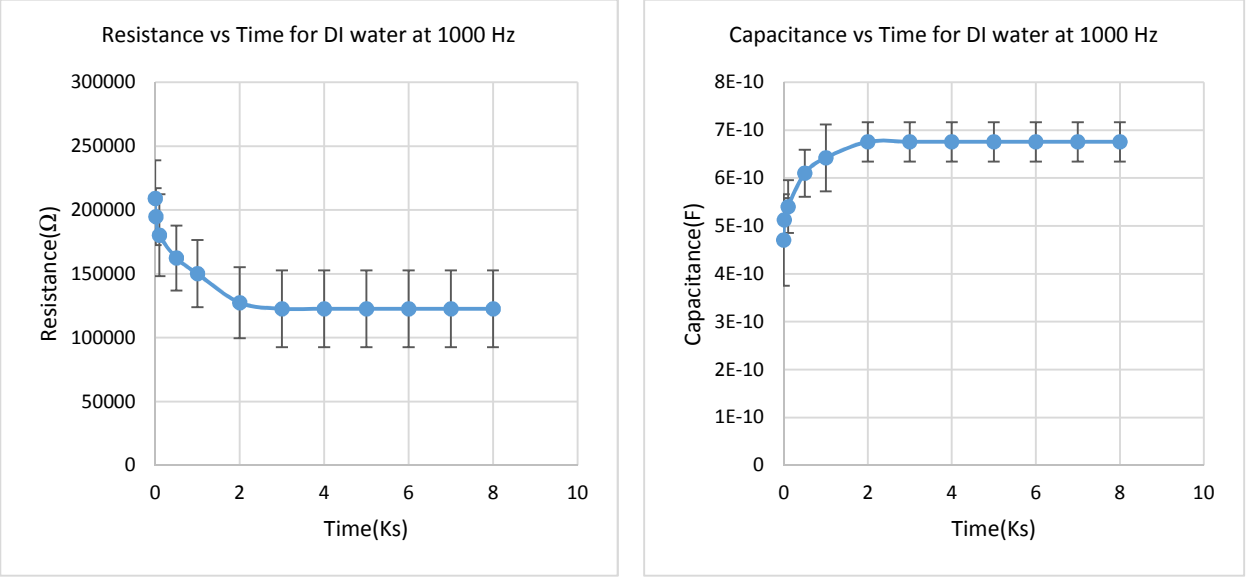

Figure 24 a,b Represents typical response of hydrophilic NPO sensor in DI water with resistance and capacitance measured in time domain

Figure 25 represents the Nyquist plot recorded at a frequency sweep from 100 Hz to 10 KHz with 100 mV (p-p) sinusoid. This plot gives us a conclusion that the sensor response is in the form of a typical parallel RC circuit with a purely resistive response after 10 KHz.

The analytes were clearly distinguished by the NPO with dominating separation from the baseline. There is a preferable gap between the baseline and the response in the analytes, namely DI water, methanol and isopropanol. A predictable response is where the alcohols and DI water have lower real and imaginary impedance compared to the organic aliphatic compounds. However n-heptane didn't show appreciable response even for the hydrophilic NPO.

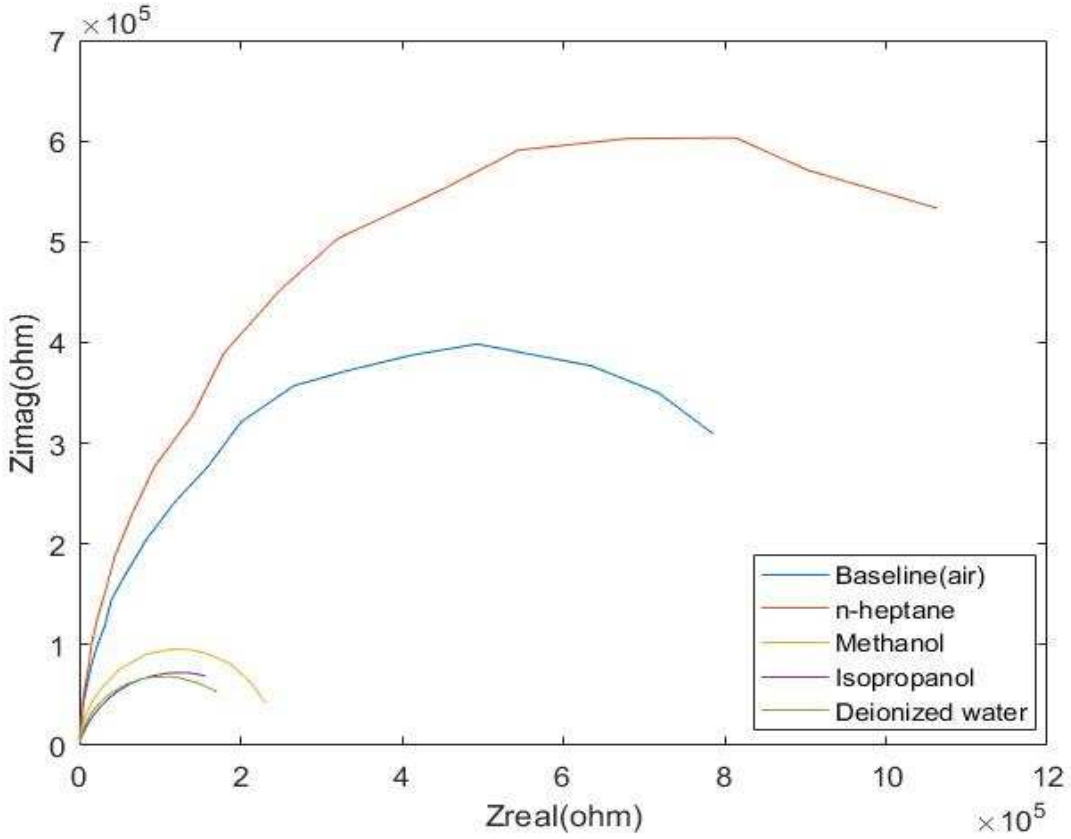

Figure 25 Nyquist plot showing frequency response of hydrophilic NPO sensor in methanol, isopropanol, n-heptane, DI water and air (baseline)

Table 1 shows the polarity index of the analytes, with water having the highest polarity and n-heptane having least polarity. Polarity index represents the ability of the compound to reach with various polar compounds. Low polarity index of n-heptane may be the cause for less response of the n-heptane onto the NPO. However Figure 26 shows the relation between the response and the polarity index: response shifts away from the baseline in analyte with higher polarity index. The graph also shows the trend with the relative permittivity, as mentioned for the AAO in the literature, with highest permittivity analytes having more shift. Figure 26 represents the Cole-Cole plot obtained for an AAO sensor on exposure to various chemical analytes.Table 2 represents the relative permittivity of the analytes.

Table 1 Value of the Polarity Index of the analytes

Name of the analyte	Polarity Index
Water	10
Methanol	5.1
Isopropanol	3.9
n-heptane	0.1

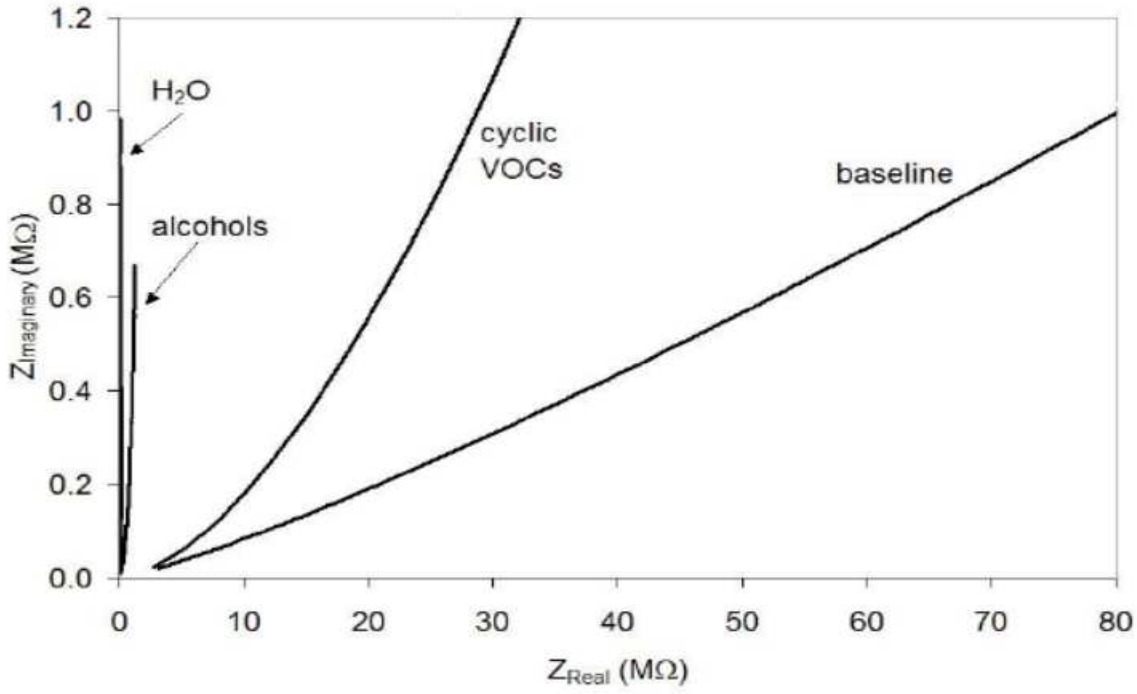

Figure 26 Cole-Cole plot of AAO sensor obtained in detecting various chemical analyte (Martin Kocanda et.al, 2009)

Table 2 Relative Permittivity Values of the Analytes

Name of the analyte	Relative permittivity
Water	78.50
Methanol	32.63
Isopropanol	16.30
n-heptane	1.93

Inspite of having least relative permittivity, n-heptane didn't show good response because of its hydrophobic nature and low polarity index, thus not forming covalent bonds with the NPO. Furthermore readings were taken during desorption of the analytes.

Figure 27 shows the desorption rate with various analytes in terms of its resistance. The rate of desorption of the analyte is directly dependent on their boiling points because if an analyte has higher boiling point then the rate of evaporation of that particular analyte will be lower. Table 3 shows the boiling point with respect to the analyte.

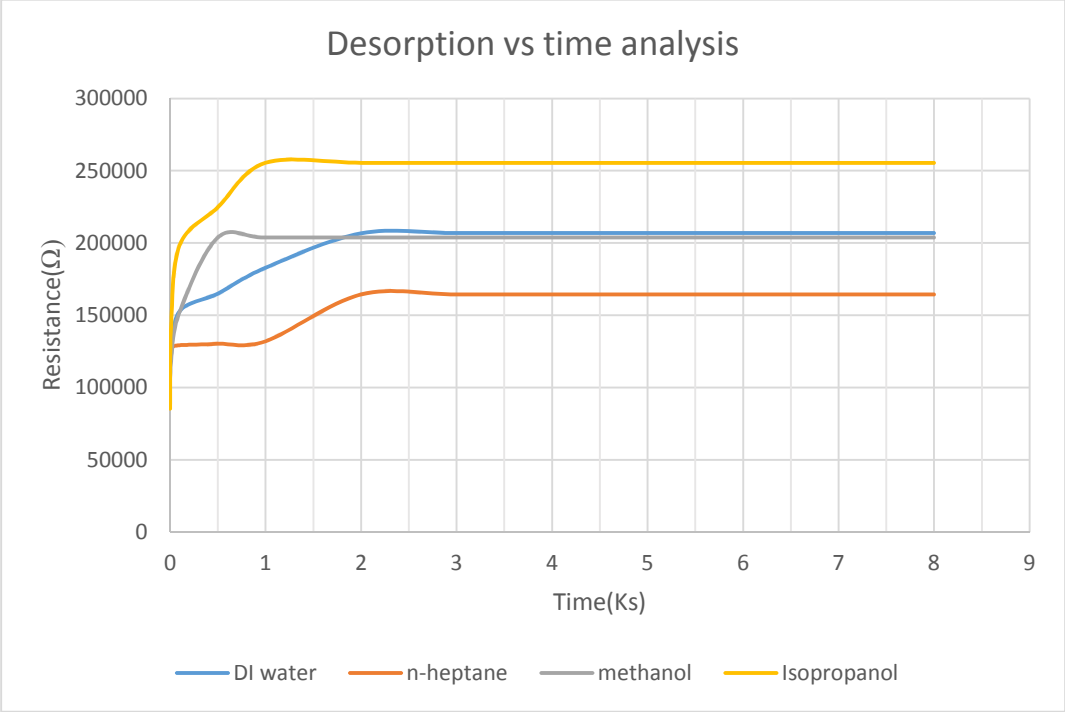

Figure 27 Analysis of the desorption rate of the plasma - treated NPO sensor in various analytes in time domain

Table 3 Boiling Points of the Analytes

Name of the analyte	Boiling point(^{o}C)
Water	100
Methanol	64.7
Isopropanol	86.20
n-heptane	98.42

As shown in Figure 27, the desorption of methanol occurs at ≈500s, isopropanol at ≈1 Ks, DI water at ≈2 Ks and n-heptane at ≈2 Ks. As both DI water and n-heptane have nearly same boiling points, their desorption is also at nearly 2 Ks. Thus it can be clearly stated that the desorption rates of the vapor analytes from the NPO surface is dependent on their respective boiling points.

3.4 Comparison of the NPO Sensor with AAO Sensor

The NPO sensor is now compared with the readings of the AAO sensor. The real and imaginary impedances of the AAO sensor are calculated using the same sensing setup used for that of the NPO. The resistance vs time and capacitance vs time graphs are obtained for the AAO sensor and are shown in Figure 28.

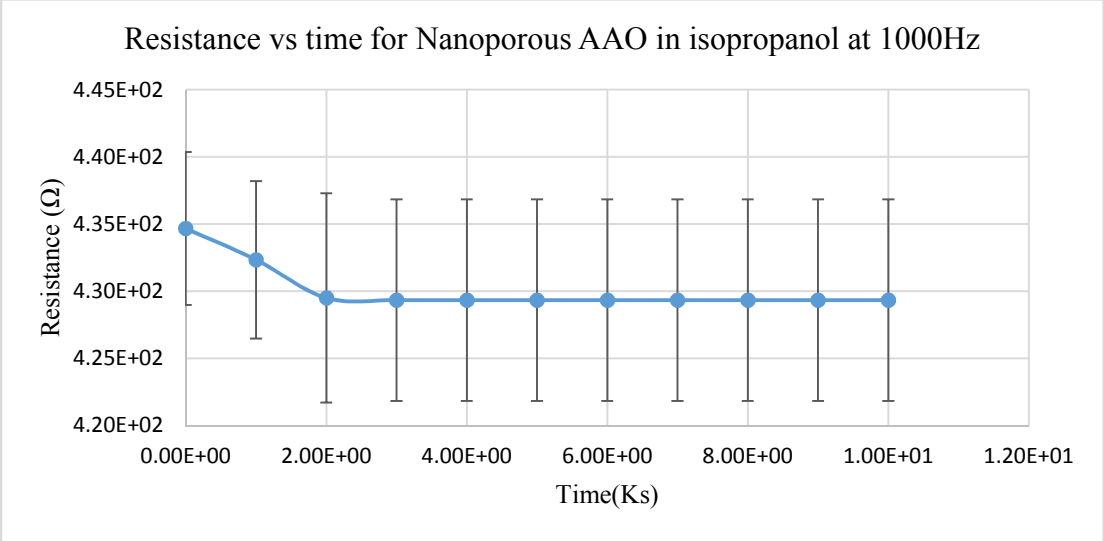

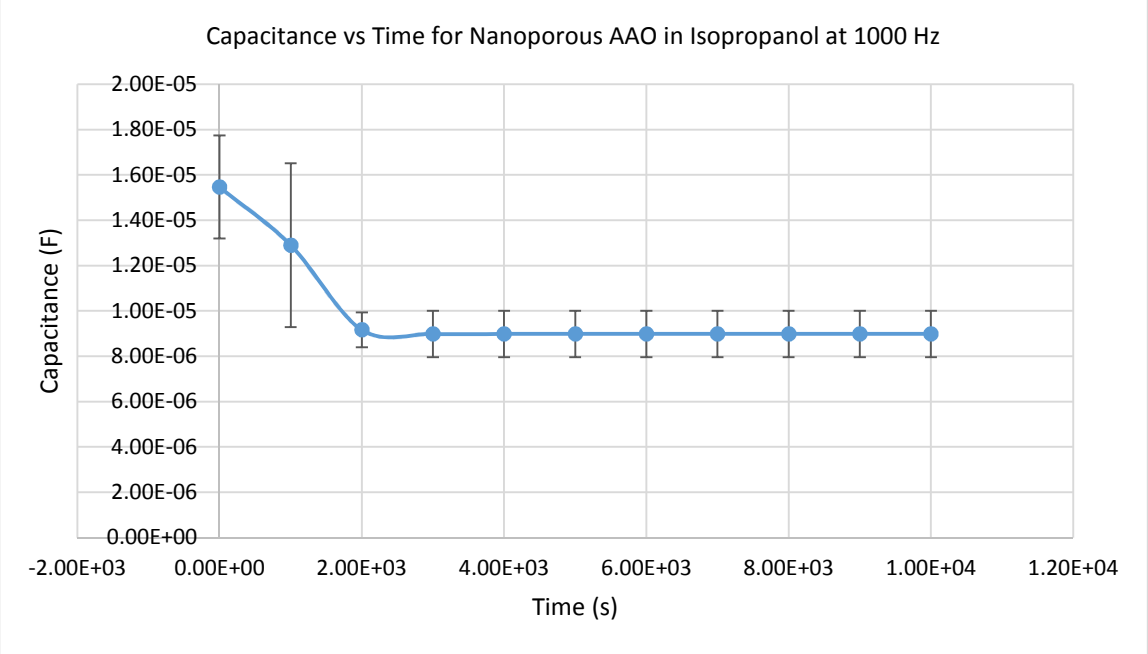

Figure 28 Time domain response of the nanoporous AAO sensor in isopropanol at 1000 Hz frequency

Figure 28 represents the resistance and capacitance in time domain of the nanoporous AAO in isopropanol at 1000 Hz frequency. When compared to that of the response of the NPO it could

be observed that the resistance of the NPO sensor is much higher compared to that of the nanoporous NPO sensor. This could be used to indicate that the NPO sensor has an ability to be a better performing sensor compared to that of the nanoporous AAO sensor.

Sensitivity of the sensor could also be calculated using the following formula:

$$\text{Sensitivity} = \frac{\text{Resistance of the sensor}}{\text{Resistance of the sensor at equilibrium in the analyte}} \times 100$$

From the above formula it could be calculated that sensitivity of the nanoporous AAO sensor in isopropanol is 101.1 % and the sensitivity of the NPO sensor in isopropanol is 300%. This proves that the NPO sensor is much more sensitive than that of the nanoporous AAO sensor with its sensitivity more than double the sensitivity of the AAO.

Chapter-4

CONCLUSION

In conclusion, we have reported on our preliminary experimentation of using nanoporous organosilicate thin films as sensor substrates. It showed that the nanoporous organosilicate films have distinguished between the various vapor - phase analytes used. However, the fabricated nanoporous organosilicate sensors (hydrophobic) exhibit sensitivity toward alcohol vapors with lower sensitivity to water vapor. But the plasma - treated nanoporous organosilicate sensor exhibit sensitivity toward alcohol vapors as well as water vapor with relatively low sensitivity toward n-heptane. The impedance spectrum (Nyquist plot) showed the hydrophilic sensor response in distinguishing of analytes depends on their relative permittivity, as in the case of nanoporous anodized aluminum oxide. It was also observed that the desorption rates of the vapor - phase analytes followed their respective boiling points. The impedance spectrum (Nyquist plot) observed depicted a typical parallel RC circuit, through which the equivalent circuit for the nanoporous organosilicate sensor could be represented as a parallel RC network.

The resistance values of the sensor recorded at different frequencies showed a very low resistance at higher frequencies, making the NPO sensor operated at lower frequencies rather than at higher frequencies. It was also observed the response of the adsorbed analytes followed their polarity: the analytes with higher polarity showed a larger change in their impedance values from the baseline.

Thus in conclusion, it could be demonstrated that the nanoporous organosilicate sensors can be used as a low-cost alternative to nanoporous anodized aluminum sensors as a chemical sensor. Future work can be done using more variety of analytes with cyclic volatile organic compounds and a mixture of compounds, analyzing if it could further discriminate from the mixture of analytes. Tunability can also be further examined, varying pore dimensions and porosity.

REFERENCES

[1] Anna C. Balazs, T. E. (2006). Nanoparticle Polymer Composites: Where Two Small Worlds Meet. *Sciece*, 1107-1110.

[2] Banica, F.-G. (2012). *Chemical Sensors and Biosensors: Fundamentals and Applications.* John Wiley & Sons.

[3] Chitra Agashe, R. C. (2008). High-yield synthesis of Nanocrystalline Tin dioxide by thermal decomposition for use in gas sensors. *The American ceramic society*.

[4] Christopher Radzik, G. K.-s. (2008). Electrical impedance response of a thick-thin film hybrid anodic nanoporous alumina sensor to methanol vapors. *International journal on smart sensing and intelligent systems*, 470-479.

[5] Dorf, R. C. (2006). *Sensors, Nanoscience, Biomedical Engineering, and Instruments.* Taylor and Francis group.

[6] F. Keller, M. S. (1953). Structural Features of Oxide Coatings on Aluminum. *Journal of the electrochemical society*, 411-419.

[7] G. Martin Kocanda, M. H.-S. (2009). Detection of cyclic volatile organic compounds using single-step anodized nanoporous alumina sensors. *IEEE sensors*, 1-6.

[8] GamryInstruments. (n.d.). Application-note. *Basics of Electrochemical Impedance spectroscopy*.

[9] Gösele, V. L. (1991). Porous silicon formation: A quantum wire effect. *Applied physics letters*, 856-858.

[10] IviumTechnologies. (n.d.). Product specification.

[11] J Hyeon-Lee, J. R. (2005). Properties of nanoporous organosilicate hybrid. *polymer international*, 772-779.

[12] Kiran Bhattacharyya, B. S. (2012). Gold nanoparticle mediated detection of circulating cancer cells. *Clinics in Laboratory Medicine*, 89-101.

[13] Licker, M. D. (2005). *Concise Encyclopedia of Science & Technology.* Mc Graw Hill.

[14] Losic, D. S. (2015). *Electrochemically Engineered Nanoporous Materials : Methods, Properties and Applications.* Springer.

[15] Mark E. Orazem, B. T. (2011). *Electrochemical Impedance Spectroscopy.* John Wiley & Sons.

[16] Morsi, Y. M. (2013). Ion Exchange Chromatography - An Overview. In D. F. Martin, *Column Chromatography* (pp. 1-30).

[17] NACL. (n.d.). *What's alumite?*

[18] Oomman K. Varghese, E. C. (2002). Room temperature ammonia and humidity sensing using highly ordered nanoporous Alumina films. pp. 91-110.

[19] *The electric world.* (1987). newyork: The W.J JoHnston Company.

[20] Venumadhav Korampally, M. Y. (2009). Entropy driven spontaneous formation of highly-porous films from polymer-nanoparticle composites. *Iopscience*, 1-7.

[21] W Lee, K. N. (2007). Self-ordering behavior of nanoporous anodic aluminum oxide (AAO) in malonic acid anodization. *Iopscience*.

[22] WOHLworks. (n.d.). Organic Analysis: Gas Chromatography.